An Oscillatory Correlation Model of Object-based Attention

Marcos G. Quiles, DeLiang Wang, Liang Zhao, Roseli A. F. Romero, and De-Shuang Huang

***Abstract*—Attention is a critical mechanism for visual scene analysis. By means of attention, it is possible to break down the analysis of a complex scene to the analysis of its parts through a selection process. Empirical studies demonstrate that attentional selection is conducted on visual objects as a whole. We present a neurocomputational model of object-based selection in the framework of oscillatory correlation. By segmenting an input scene and integrating the segments with their conspicuity obtained from a saliency map, the model selects salient objects rather than salient locations. The proposed system is composed of three modules: a saliency map providing saliency values of image locations, image segmentation for breaking the input scene into a set of objects, and object selection which allows one of the objects of the scene to be selected at a time. This object selection system has been applied to real images and the simulation results show its effectiveness.**

I. Introduction

The perceptual mechanism of selecting a part of the visual input for conscious analysis is called selective visual attention, and it is a mechanism that is fundamentally important for the survival of an organism [3], [25]. Visual attention is thought to involve two aspects [25]. The first one is called bottom-up (or stimulus-driven) attention that is based on analyzing stimulus characteristics of the input scene. The second aspect is top-down control (or goal-driven attention) that is influenced by the intention of the viewer, like looking for a specific thing.

Attention can be directed to spatial locations, visual features, or objects (for a review see [4]). Recent behavioral and neurophysiological evidence establishes that the selection of objects plays a central role in primate vision [13], [14], [15], [22]. It is believed that a preattentive process, in the form of perceptual organization, is performed unconsciously by the brain. This process is responsible for segmenting the visual scene into a set of objects which then act as wholes in the competition for attentional selection [3]. Perceptual organization has been extensively studied in Gestalt psychology where it is emphasized that the visual world is perceived as an agglomeration of well structured objects, not as an unorganized collection of pixels.

Due to the competitive nature of visual selection, most of the neural models are based on winner-take-all (WTA) networks [6], [7], [10]. Through neural competition, a WTA network selects one neuron, the winner, in response to a given input [1]. In this way, a pixel or location, not an object, of the scene is selected. These visual selection models correspond to location-based theories of visual attention, but not object-based theories.

In order to develop a neural model of visual selection that is object-based, one has to address how to group the elements, or features, of a visual scene into a set of coherent objects. The problem of how sensory elements of a scene are combined together to form perceptual objects in the brain is known as the *binding problem* [18]. Von der Malsburg proposed *temporal correlation theory* to address the binding problem [18]. The theory asserts that objects are represented by the temporal correlation of the firing activities of spatially distributed neurons coding different object features. A natural way of encoding temporal correlation is using synchronization of neural oscillators [17], [19], [21]. This form of temporal correlation is called *oscillatory correlation* [17] whereby oscillators that encode different features of the same object are synchronized and those that encode different objects are desynchronized. The oscillatory correlation theory has been applied to various tasks of scene analysis (see [21] for an extensive review).

Although oscillation-based models for visual attention have been studied for years [12], the first attempt to perform object selection using oscillatory correlation was made by Wang [20]. This study achieves size-based object selection based on LEGION (Locally Excitatory Globally Inhibitory Oscillator Network) and a slow inhibition mechanism. However, the model considers just object size in competition. Size-based selection was also considered by Kazanovich and Borisyuk [9] where the frequency and amplitude of oscillators are used to perform selection. A different object-based model for visual attention was proposed in [16]. Although this model performs object-based selection, it assumes that perceptual organization has already been done. An oscillatory correlation model has also been developed for auditory selective attention [24].

Here we propose an object-based visual selection model with three major components. First, a saliency map is employed to calculate point-wise conspicuity over the input scene. This saliency map is intended to simulate feature and location based aspects of visual attention. Second, the LEGION network is used to segment the input image, and this network is intended to perform the task of perceptual organization. Third, an object-based selection network is proposed. This selection network chooses the most salient object using an *object-saliency map* created by integrating the results from the saliency map and LEGION segmentation. Moreover, our selection network is able to shift the focus of

M. G. Quiles, L. Zhao, and R. A. F. Romero are with the Department of Computer Science, Institute of Mathematics and Computer Science (ICMC), University of São Paulo (USP), São Carlos, SP, Brazil (e-mail: quiles, zhao, rafrance@icmc.usp.br).

D. L. Wang is with the Department of Computer Science & Engineering and Center for Cognitive Science, The Ohio State University, Columbus, OH 43210 USA (e-mail: dwang@cse.ohio-state.edu).

D.-S. Huang is with the Intelligent Computing Lab, Hefei Institute of Intelligent Machines, Chinese Academy of Sciences, P.O.Box 1130, Hefei, Anhui 230031, China (email: dshuang@iim.ac.cn).

978-1-4244-3553-1/09/$25.00 ©2009 IEEE

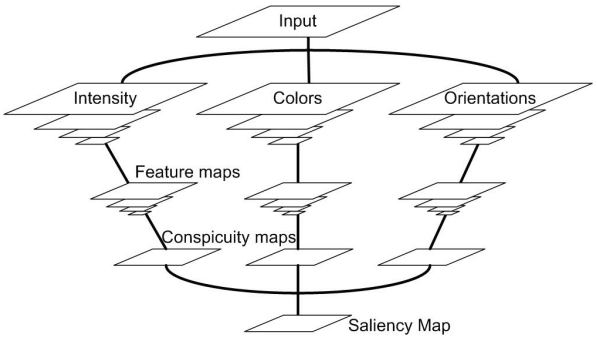

Fig. 1. Flowchart of a saliency map [7].

attention from one object to the next.

This paper is organized as follows. In Section II, an overview of the saliency map and LEGION segmentation is presented. Section III describes the selection layer of the system. Evaluation results are presented in Section IV. Finally, Section V offers a few concluding remarks.

II. Background

A. Saliency Map

To compute the saliency we use the saliency map proposed in [7], [10]. This saliency map mimics the properties of early vision in primates and is based on the idea that a unique map is used to control the deployment of attention [6], [10].

The saliency map is an explicit two-dimensional map responsible for encoding the saliency over all points of the visual scene. It focuses on the role of local feature contrast in guiding attention [6], [7]. Despite its simple architecture based on feedforward feature-extraction mechanisms, this model has proved to have robust performance when dealing with complex scenes and it achieves some qualitative results matching human visual search [6].

Generally speaking, the saliency map is produced in the following way. First, a set of maps representing primary features, such as color and orientation, are extracted from the input scene. After that, in order to model the center-surround receptive fields, operations are performed over different spatial scales of those maps. This process followed by a normalization operator results in a new set of maps called *feature maps*. Next, feature maps are combined into a set of *conspicuity maps*. Finally, a linear combination of conspicuity maps results in the *saliency map*. A flowchart of this process is shown in Figure 1 and a formal description of the process can be found in [7].

The saliency map S^m is used to compute the object-saliency map described in Section III.

B. Image Segmentation

The scene segmentation model [23] is an extension of the LEGION model [17]. The basic unit of LEGION is a relaxation oscillator defined as a feedback loop between an excitatory variable x_i and an inhibitory variable y_i [17]:

$$\dot{x}_i = 3x_i - x_i^3 + 2 - y_i + \mathcal{I}_i + S_i + \rho \quad (1a)$$

$$\dot{y}_i = \epsilon(\alpha(1 + \tanh(x_i/\beta)) - y_i) \quad (1b)$$

where $\mathcal{I}_i$ represents the external stimulation, S_i the input from neighboring oscillators in the network, and ρ denotes the amplitude of Gaussian noise. Parameter ϵ is a small positive number.

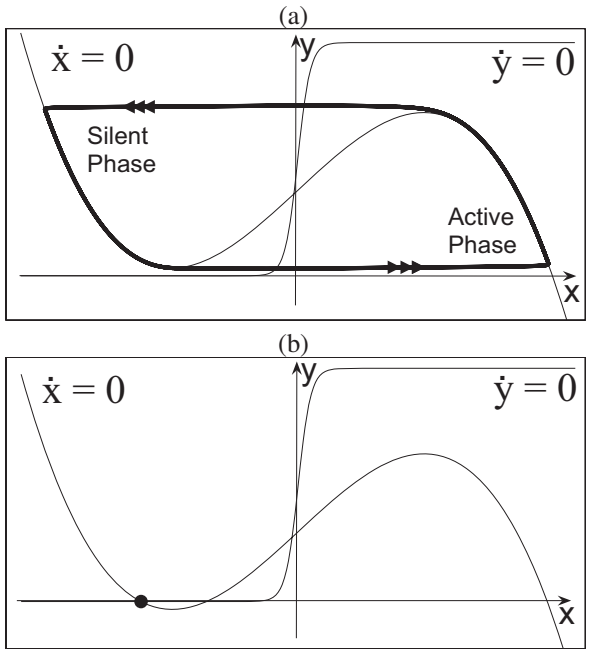

Fig. 2. Dynamics of a single relaxation oscillator. (a) Behavior of an enabled oscillator. A limit cycle trajectory is represented by a bold curve and the arrows indicate the motion direction. (b) Behavior of an excitable oscillator. In this case, a stable fixed point is observed indicated by the dot.

Figure 2 shows the nullclines and the trajectories of a single oscillator defined in Eq. (1), where the x-nullcline is a cubic function and the y-nullcline is a sigmoid function. If the total stimulation received by the oscillator, $\mathcal{I}_i+S_i+\rho > 0$, the nullclines intersect at just one point at the middle branch of the cubic. In this case, the oscillator is said to be *enabled* and a stable cycle limit is observed (see Fig. 2(a)). The periodic orbit alternates between an *active phase* and a *silent phase*, which correspond to high and low x values, respectively. The transition between the two phases occurs rapidly in comparison with the motion within each phase, thus referred to as *jumping*. The parameter α controls how much time the oscillator spends in these two phases. When the total input $\mathcal{I}_i + S_i + \rho < 0$, the two nullclines of Eq. (1) intersect at a stable fixed point on the left branch of the cubic (see Fig. 2(b)). In this case, no oscillation is observed. As the oscillator can be induced to oscillate by external stimulation, such a state is called *excitable*. The parameter β controls the steepness of the sigmoid which is normally set to a small value in order to make the sigmoid approach a step function [17].

To perform image segmentation on real images, a lateral potential term is introduced to distinguish between major

regions and noisy fragments [23]. This mechanism can be explained as follows. If oscillator i lies in the center of a homogeneous image region, it is able to receive a large input from its neighbors; in this case it is defined as a *leader*. On the other hand, if it corresponds to an isolated fragment of the image, it does not receive a large input from its neighborhood and hence cannot become a leader. Based on this idea, only blocks which have at least one leader are allowed to oscillate.

The connection term S_i of Eq. (1a) is defined as follows:

$$S_i = \sum_{k \in N(i)} W_{ik} H(x_k - \theta_x) - W_z H(z - \theta_z) \qquad (2)$$

where W_{ik} defines the connection weight from oscillator k to i and $N(i)$ represents a set of oscillators that comprises the neighborhood of i [23]. H represents the Heaviside function defined as $H(v) = 1$ if $v \geq 0$ and $H(v) = 0$ otherwise. θ_x and θ_z are thresholds.

W_z in Eq. (2) defines the inhibition weight associated with the global inhibitor z. The dynamics of z is defined as:

$$\dot{z} = \phi \left(\sum_k H(x_k - \theta_x) - z \right) \qquad (3)$$

where ϕ is a parameter that controls how fast the global inhibitor reacts to the stimulation received from the oscillators. Note that z approaches the number of oscillators in the active phase, and will be used to represent the size of each synchronized oscillator block (segment).

Based on the LEGION dynamics described above, Wang and Terman [23] developed a computer algorithm that follows the main aspects observed on the numerical simulations of the Equations (1)-(3). Detailed description of this algorithm can be found in [23].

III. Model Description

Figure 3 shows a flowchart of our model. First, an input image feeds the image segmentation and saliency map modules. Second, the segmentation result and the saliency map are combined to build an object-saliency map that feeds the object selection module. Third, the object selection module selects the most salient object and suppresses all the others. Finally, the Inhibition of Return (IoR) mechanism is included in the object selection module that inhibits the previously selected object in order to allow the next most salient object to be selected.

The following sections describe how the object-saliency map is created and how object selection works.

A. Object-Saliency Map

The object-saliency map, S, is responsible for providing the level of saliency of each object in the input scene. This map differs from S^m which represents the saliency of each pixel. For each segment produced by the segmentation layer, its average saliency is calculated from all the corresponding points in S^m:

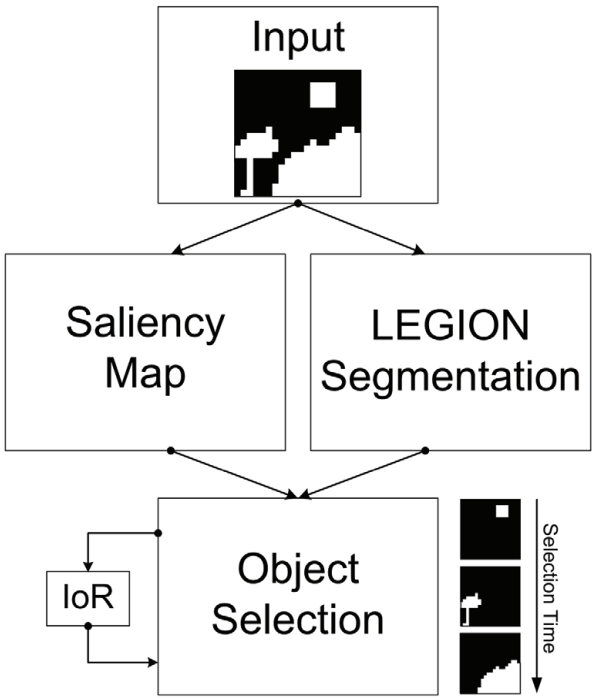

Fig. 3. Diagram of the proposed object selection model, which is composed a saliency map, a LEGION segmentation layer, and an object selection layer that includes an inhibition-of-return (IoR) mechanism. Arrows indicate the computational flow of the system. The images shown below the selection layer illustrates a sequence of the objects selected.

$$S(i) = \frac{\sum_{j \in O(i)} S^m(j)}{|O(i)|} \sqrt[5]{\frac{|O(i)|}{|O_M|}} \qquad (4)$$

where $O(i)$ is the set of all pixels grouped with pixel i in the same segment; $S^m(j)$ is value of the saliency map at pixel j; $|O(i)|$ is the size of $O(i)$; $|O_M|$ is the size of the largest segment in the input image; and the 5^{th}-root function is used to moderate the saliency of relatively small segments.

As described above, to calculate the object-saliency map S we utilize the results generated by the previous layers. Thus, the segmentation process must be concluded before selection can happen. An interesting property of the segmentation algorithm based on LEGION is that the process is completed when every leader has jumped up once [23]. In this way, we can generate the object-saliency map and perform visual selection after the segmentation process is completed.

B. Object Selection

The object selection network is an extension of the LEGION model following the ideas developed in [20] where a fast and a slow inhibitor are responsible for desynchronizing the objects and selecting the one of them, respectively.

This network follows the dynamics described in Section II-B. The main differences between our network for object selection and LEGION for image segmentation are the presence of the slow inhibitor, the introduction of the IoR mechanisms, and how the external stimulation is defined.

Here, each oscillator is connected to its eight nearest neighbors as follows. If two neighboring oscillators have their corresponding oscillators in the segmentation layer synchronized, they are connected. On the other hand, if the corresponding oscillators in the segmentation layer do not belong the same object (i.e. desynchronized), the connection between the two oscillators in the object selection layer is set to zero. Thus, the objects formed in the LEGION layer are directly transported to the object selection layer.

The external stimulation $\mathcal{I}_i$ is defined as follows:

$$\mathcal{I}_i = V_i H(S(i) - Cz_s) H(r_i - \theta_z) \tag{5}$$

where V_i is set to a high value if the corresponding oscillator i in the segmentation layer is enabled. Otherwise, V_i is set to a low value. In this way, oscillators in the object selection layer corresponding to a segment in LEGION assume high values of V, whereas oscillators representing noisy fragments (the background) have a low V value. C is a parameter that controls the number of objects that can be selected at a time [20]. The variable r_i models the IoR component of each oscillator described by the following equation:

$$\dot{r}_i = -\omega r_i H(x_i - \theta_x) \tag{6}$$

Initially, for each oscillator i, r_i is set to 1. Every time an oscillator jumps to the active phase, its r_i value is reduced following Eq. (6). After a number of cycles controlled by parameter ω, r_i approaches zero. Thus, the second Heaviside function of Eq. (5) returns zero and the oscillator is inhibited. Due to the presence of the IoR, the selection network is allowed to select the next most salient object, which resembles attentional shifts in visual perception [6].

The dynamics of the slow inhibitor of Eq. (5) is defined as:

$$\dot{z}_s = \psi \left[\sum_k \frac{S(k) H(x_k - \theta_x)}{|O(k)|} - z_s \right]^+ - \mu \epsilon z_s \tag{7}$$

where the function $[v]^+ = v$ if $v \geq 0$ and 0 otherwise. The parameters ψ and μ are on the order of 1. The slow inhibitor is characterized by a fast rise and a slow decay owing to the small value of the relaxation parameter ϵ. The selection process is produced by the Heaviside function and the slow inhibitor which allows to become active just the oscillators with $S(i) \geq Cz_s$. Thus, by setting a proper value of C as defined in [20], only the object with the highest value of $S(i)$ is allowed to oscillate, i.e. to be selected.

Once we have the saliency of all the objects, we can use these values to determine which object oscillates so as to avoid the time-consuming competition for selection. To achieve this behavior, the initial value of y_i (Eq. 1b) is set according to its object-saliency value in the following way:

$$y_i = 2\alpha(1 - S(i)) + V_i \tag{8}$$

The overall behavior of our model can be understood as follows. The saliency map calculates the saliency of all pixels. In parallel, the LEGION layer segregates the input image into a set of segments. After that, the object-saliency map is generated based on Eq. (4). This map feeds the object selection layer. In Eq. (5), the first Heaviside plays the role of object selection and the second the IoR. If the first Heaviside returns 0, i.e. the object saliency value that feeds the oscillator does not exceed the level of the slow inhibitor, the object is inhibited. On the other hand, if the object saliency value that feeds a block of oscillators exceeds slow inhibition, the object represented by them is selected. At the same time, the slow inhibitor assumes a new value through Eq. (7) which represents the object saliency of the currently active segment. As a result, other objects with smaller object saliency values are prevented from being selected.

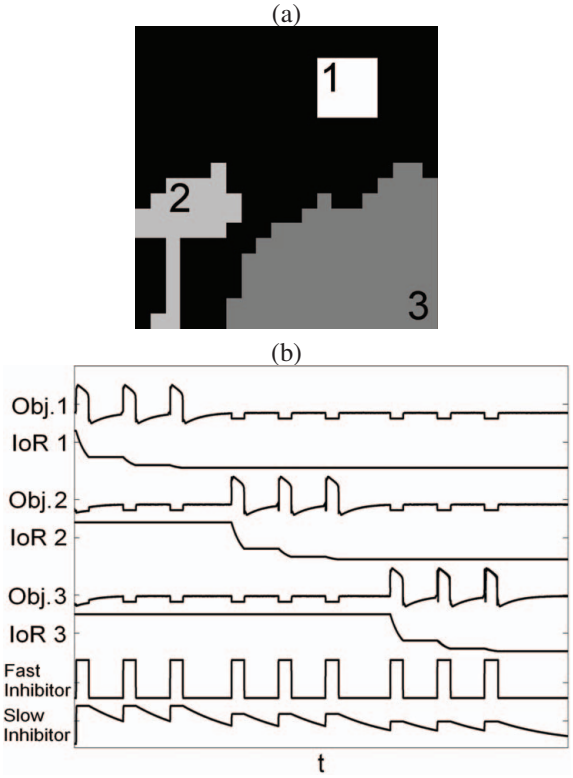

Fig. 4. Illustration of the object selection process. The selection network is integrated using the fourth-order Runge-Kutta method. (a) Object-saliency map showing three objects: a square (1), a left object (2) and a lower-right object (3). (b) Activity of each oscillator block (indicated by an object number) and its corresponding IoR, plus the activity traces of the fast and the slow inhibitor.

Once a block is oscillating, the IoR mechanism takes effect and each oscillator i within that block has its r_i reduced by Eq. (6). After a few cycles, r_i approaches zero. Thus, the second Heaviside of Eq. (5) returns 0, which represents the inhibition of oscillator i and consequently the inhibition of the whole segment. Following the inhibition of this object, the slow inhibitor has its value decreased by Eq. (7) and the next object is selected. This behavior is shown in Fig. 4.

IV. Simulation Results

Before presenting simulation results, we first describe the parameters used in the modules. In the saliency map module

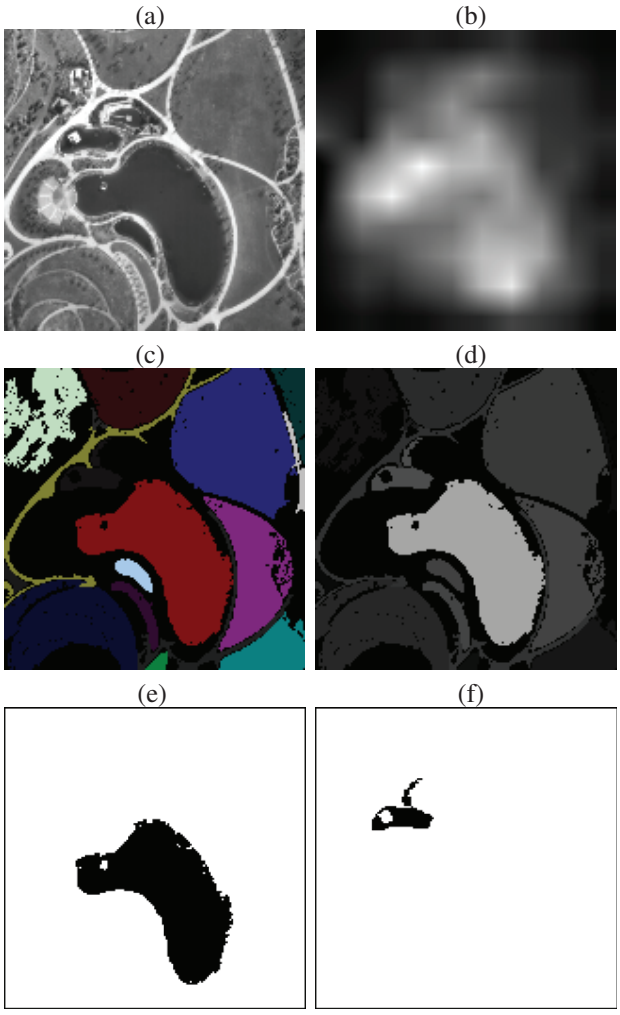

Fig. 5. Object selection result for a gray level image. (a) Input image which is an aerial image with 160×160 pixels. (b) Saliency map. (c) Result of LEGION segmentation, where each segment is represented by a distinct color. (d) Object-saliency map. (e) First object selected. (f) Second object selected.

we apply the same parameter values used in [7]. Image segmentation is performed by the algorithm presented in [23]. The coupling strength W_{ij} between two neighbor oscillators is set according to their similarity using the following rule. For gray level images,

$$W_{ij} = I_M/(1 + |I_i - I_j|) \tag{9}$$

For color images,

$$W_{ij} = I_M/\left(1 + \sum_{h\in\{r,g,b\}} |h_i - h_j|\right) \tag{10}$$

where I_M is the maximum value of the channels I, r, g, and b. In our simulations, this value is set to 255. I_i is the gray level of pixel i. h_i represents the color channel (r, g, and b) of a color pixel i.

The object selection network presented in Section III-B is integrated by using the fast numerical method of singular limit which allows for simulating large networks of relaxation oscillators [11]. The following parameter values are used for integrating the selection network by the singular limit method: $\alpha = 6.5$, $W_z = 0.7$, and $\mu = 0.125$. All the other parameters are not necessary when solving the equations using this method. $C = 1.65$ is used for all the experiments.

Figure 5(a) shows the first input figure. Figure 5(b) presents the saliency map from Fig. 5(a) where brighter pixels indicate higher saliency points. Here, by using $W_z = 20$ the LEGION network produces 17 segments as shown in Fig 5(c). Based on the results from the saliency map (Fig. 5(b)) and LEGION (Fig. 5(c)), the object-saliency map is shown in Figure 5(d). In this figure, a brighter object indicates a higher saliency one. This map feeds the object selection network which first chooses the most salient object shown in Figure 5(e), representing a lake in the central part of the scene. After that, due to the IoR mechanism described in Section III-B, the oscillators representing the first selected object are inhibited allowing the system to select the second most salient object which is shown in Fig. 5(f). In all the simulations presented in this paper, only the first and the second selected objects are shown to illustrate the selection process.

Next, we present results on color images in Figures 6 and 7. In Figure 6(a), due to the high contrast of the beetle with its background composed of mostly yellow and green things, the beetle seems to be the first object to pop out from the scene for a human observer. This percept agrees with the result from our object-saliency map in Fig 6(b), where the segment corresponding to the beetle is the brightest. As we can see in Fig. 6(c), the first object to be selected is indeed the beetle. Figure 7 presents a simulation of a scene where the most salient object appears to a boat to a human observer. Again, due to its high contrast with background objects, the boat is selected by our system as the first object (see Fig. 7(c)).

Other simulations with gray and color images have been conducted, and results with similar quality have been obtained. In these simulations, the objects selected by our system appear to match perceptual observations.

V. Concluding Remarks

Object based attention has received empirical support [13], [14], [15], [22]. In this paper we have presented an object selection model based on oscillatory correlation theory. This model integrates several modules: A saliency map, which calculates the saliency values of all the locations of the input scene, a LEGION network for segmenting the scene into a set of segments or objects, and an object selection network for selecting the most salient object of the scene. Modeling visual attention with an oscillator network is motivated by physiological studies suggesting that synchronous activity plays a fundamental role in solving the binding problem and visual attention [5], [8], [18]. In contrast to previous computational models of location-based visual attention, our model, due to the use of an image segmentation layer, is able

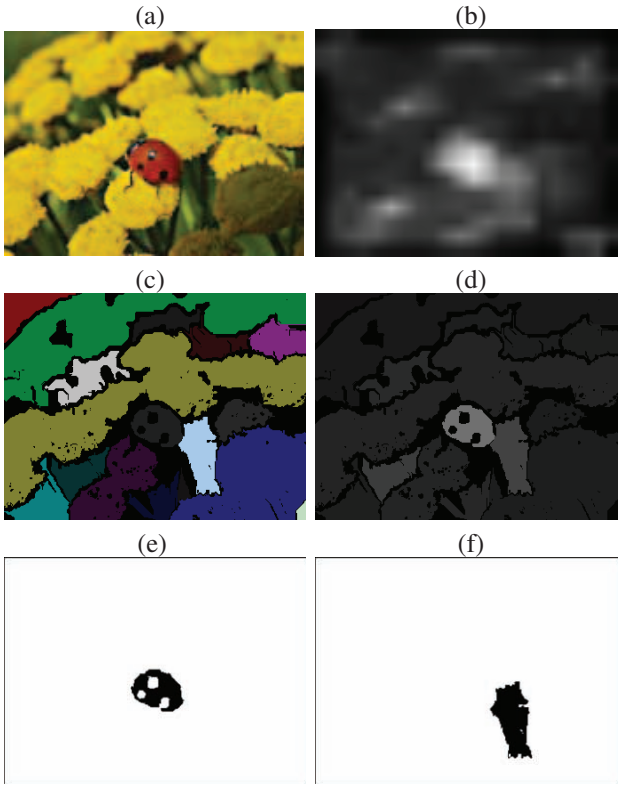

Fig. 6. Object selection result for a color image. (a) Input image with 351×256 pixels. (b) Saliency map. (c) Result of LEGION segmentation, where each segment is represented by a distinct color. (d) Object-saliency map. (e) First object selected. (f) Second object selected.

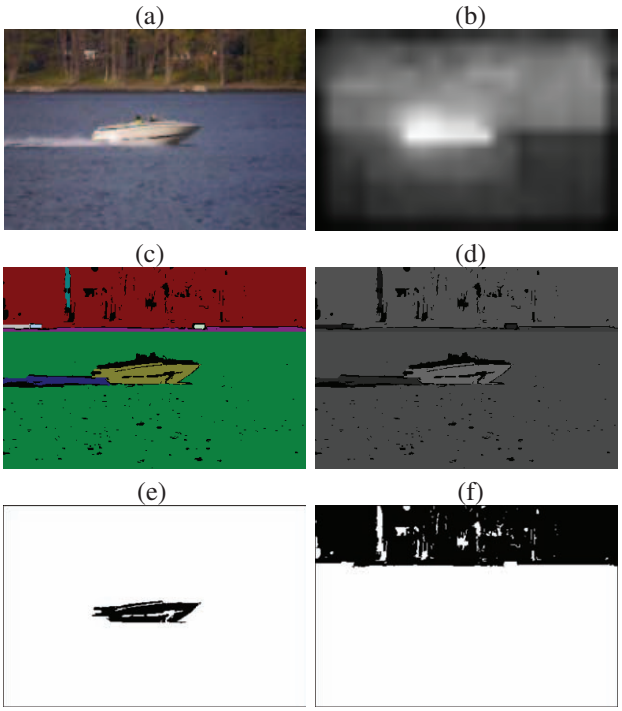

Fig. 7. Object selection result for a color image. (a) Input image with 385×256 pixels. (b) Saliency map. (c) Result of LEGION segmentation, where each segment is represented by a distinct color. (d) Object-saliency map. (e) First object selected. (f) Second object selected.

to deal with objects directly. By integrating the saliency map, the segmentation layer, and the IoR mechanism, our selection network can select a set of objects sequentially according to their saliency.

Our model has several limitations that need to be addressed in future work. The proposed system only addresses bottom-up aspects of attentional selection, and top-down guidance of attention is not modeled. Incorporation of other visual features, such as motion and object contour, among others, could further enhance the performance of the system. Finally, it should also be stated that even though the architecture of our model is motivated by experimental studies of visual attention, our model does not simulate psychophysical data in a quantitative way. Neurocomputational models have been developed to simulate perceptual data of visual attention (see [2] among others).

Acknowledgment

This work was undertaken while M.G.Q. was a visiting scholar in the Perception and Neurodynamics Lab at The Ohio State University. M.G.Q. was supported by the São Paulo State Research Foundation (FAPESP). D.L.W. was supported in part by an NGI University Research Initiatives grant and the K.C. Wong Education Foundation (Hong Kong). L.Z. and R.A.F.R. were supported by the Brazilian National Research Council (CNPq).

References

[1] M. A. Arbib, *Handbook of brain theory and Neural Networks*, 2nd ed. Cambridge, MA: MIT Press, 2003.

[2] S. Corchs and G. Deco, "A neurodynamical model for selective visual attention using oscillators," *Neural Networks*, vol. 14, pp. 981–990, 2001.

[3] R. Desimone and J. Duncan, "Neural mechanisms of selective visual attention," *Annual Review of Neuroscience*, vol. 18, pp. 193–222, 1995.

[4] H. E. Egeth and S. Yantis, "Visual attention: control, representation, and time course," *Annual Review of Psychology*, vol. 48, pp. 269–297, 1997.

[5] P. Fries, J. H. Reynolds, A. E. Rorie, and R. Desimone, "Modulation of oscillatory neuronal synchronization by selective visual attention," *Science*, vol. 291, pp. 1560–1563, 2001.

[6] L. Itti and C. Koch, "Computational modelling of visual attention," *Nature Reviews Neuroscience*, vol. 2, pp. 194–203, 2001.

[7] L. Itti, C. Koch, and E. Niebur, "A mode of saliency-based visual attention for rapid scene analysis," *IEEE Transactions on Pattern Analysis and Machine Intelligence*, vol. 20, no. 11, pp. 1254–1259, 1998.

[8] W. J. Jermakowicz and V. A. Casagrande, "Neural networks a century after cajal," *Brain Research Reviews*, vol. 55, no. 2, pp. 264–284, 2007.

[9] Y. Kazanovich and R. Borisyuk, "Object selection by an oscillatory neural network," *Biosystems*, vol. 67, pp. 103–111, 2002.

[10] C. Koch and S. Ullman, "Shifts in selective visual attention: Towards the underlying neural circuitry," *Human Neurobiology*, vol. 4, pp. 219–227, 1985.

[11] P. S. Linsay and D. L. Wang, "Fast numerical integration of relaxation oscillator networks based on singular limit solution," *IEEE Transactions on Neural Networks*, vol. 9, no. 3, pp. 523–532, 1998.

[12] E. Niebur, C. Koch, and C. Rosin, "An oscillation-based model for the neuronal basis of attention," *Vision Research*, vol. 33, pp. 2789–2802, 1993.

[13] K. M. O'Craven, P. E. Downing, and N. Kanwisher, "fmri evidence for objects as the units of attentional selection," *Nature*, vol. 401, pp. 584–587, 1999.

[14] P. R. Roelfsema, V. A. F. Lamme, and H. Spekreijse, "Object-based attention in the primary visual cortex of the macaque monkey," *Nature*, vol. 395, pp. 376–381, 1998.
[15] B. G. Shinn-Cunningham, "Object-based auditory and visual attention," *Trends in Cognitive Sciences*, vol. 12, no. 5, pp. 182–186, 2008.
[16] Y. Sun and R. Fisher, "Object-based visual attention for computer vision," *Artificial Intelligence*, vol. 146, pp. 77–123, 2003.
[17] D. Terman and D. L. Wang, "Global competition and local cooperation in a network of neural oscillators," *Physica D*, vol. 81, pp. 148–176, 1995.
[18] C. von der Malsburg, "The correlation theory of brain function," Internal report 81-2: Max-Planck Institute for Biophysical Chemistry, Göttingen, Germany, Tech. Rep., 1981.
[19] C. von der Malsburg and W. Schneider, "A neural cocktail-party processor," *Biological Cybernetics*, vol. 54, pp. 29–40, 1986.
[20] D. L. Wang, "Object selection based on oscillatory correlation," *Neural Networks*, vol. 12, pp. 579–592, 1999.
[21] ——, "The time dimension for scene analysis," *IEEE Transactions on Neural Networks*, vol. 16, no. 6, pp. 1401–1426, 2005.
[22] D. L. Wang, A. Kristjansson, and K. Nakayama, "Efficient visual search without top-down or bottom-up guidance," *Perception & Psychophysics*, vol. 67, no. 2, pp. 239–253, 2005.
[23] D. L. Wang and D. Terman, "Image segmentation based on oscillatory correlation," *Neural Computation*, vol. 9, pp. 805–836, 1997.
[24] S. N. Wrigley and G. J. Brown, "A computational model of auditory selective attention," *IEEE Transactions on Neural Networks*, vol. 15, no. 5, pp. 1151–1163, 2004.
[25] S. Yantis, *Attention*. Psychology Press, London, 1998, ch. Control of visual attention, pp. 223–256.